THESIS

IMPACT OF FORCED AND INTERNAL CLIMATE VARIABILITY ON CHANGES IN CONVECTIVE ENVIRONMENTS OVER THE EASTERN UNITED STATES

Submitted by

Megan E. Franke

Department of Atmospheric Science

In partial fulfillment of the requirements

For the Degree of Master of Science

Colorado State University

Fort Collins, Colorado

Summer 2022

Master's Committee:

Advisor: James W. Hurrell

Kristen L. Rasmussen
Nathan D. Mueller

ABSTRACT

IMPACT OF FORCED AND INTERNAL CLIMATE VARIABILITY ON CHANGES IN CONVECTIVE ENVIRONMENTS OVER THE EASTERN UNITED STATES

Hazards from convective weather and severe storms pose a serious threat to the continental United States (CONUS). Previous studies have examined how future projected changes in climate might impact the frequency and intensity of severe weather using simulations with both convection-permitting regional models and coarser-grid Earth system models. However, most of these studies have been limited to single representations of the future climate state with little insight into the uncertainty of how the population of convective storms may change. To more thoroughly explore this aspect, we utilize a large-ensemble of climate model simulations to investigate the forced response and how it may be modulated by internal variability. Specifically, we use daily data from an ensemble of 50 climate simulations with the most recent version of the Community Earth System Model (CESM) to examine changes in the severe weather environment over the eastern CONUS during boreal spring from 1870-2100. Our results indicate that the large-scale convective environment changed little between 1870 and 1990, but from then throughout the 21st century, convective available potential energy increases while 0-6 km vertical wind shear and convective inhibition decreases (increased stability). While the forced changes in these variables are robust both in space and time, we show that they are likely to be modified significantly by internal climate variability. This effect can either act to significantly enhance the forced response or conversely, suppress it in such a way that produces changes in the convective environment that are opposite to the forced response. The time evolution of bivariate distributions of convective indices illustrates that future springtime convective environments over the eastern CONUS will be characterized by relatively less frequent, but deeper and more intense convection. Future convective environments will also be less supportive of the most severe convective modes and their associated hazards.

ACKNOWLEDGEMENTS

I would like to thank Dr. James W. Hurrell for believing in me and supporting me through the completion of this thesis. I would also like to thank Dr. Kristen L. Rasmussen for her input and expertise in the mesoscale processes included in this work, as well as Dr. Lantao Sun for always being willing to help me with coding, especially in the very beginning. I have grown immensely in this process thanks to you all. Lastly, thank you to Dr. Nathan D. Mueller for his time and role on my graduate committee.

DEDICATION

This thesis is dedicated to my Grandma Beth,

who has always inspired me to go after my dreams.

TABLE OF CONTENTS

LIST OF FIGURES

Chapter 1

Introduction

Few places around the globe experience extreme severe weather like the United States. Particularly over the central and eastern U.S., the peak in severe weather is largely due to synoptic-scale interactions with the Rocky Mountains. During the boreal spring season, the Bermuda High, as well as the nocturnal Great Plains Low-Level Jet (GPLLJ), enhances a southerly flow of warm, moist air from the Gulf of Mexico into the Great Plains (Pitchford and London 1962; Higgins et al. 1997; Li et al. 2011). This moist air, trapped by the mountain range to the west, creates a thick gradient between the dry, western desert air and provides the necessary ingredients for high convective energy downstream. In addition, the terrain of the Rockies helps to produce a midlevel capping inversion as the hot, dry mixed layer is advected off the elevated plateaus, and then becomes further enhanced as the climatological westerly flow aloft descends the lee-side of the mountains (Carlson et al. 1983). This inversion, also typically seen downstream of the Rockies, suppresses convective activity and further facilitates the daily accumulation of convective energy to build to extreme levels before the inversion is broken and enhanced lifting can occur, allowing for deep convection to ensue.

In the year 2021 alone, 20 destructive meteorological events occurred each resulting in $1 billion or more of damages, 11 of which were due to severe weather events including hazards such as tornadoes, large hail, and strong winds (NCEI, 2021). Records from the National Climatic Data Center indicate that, over the last decade, the occurrence of billion-dollar severe weather events has more than doubled. Additionally, the Intergovernmental Panel on Climate Change (IPCC) has noted with high confidence that models consistently project changes in climate that support an increase in the frequency and intensity of severe weather (IPCC, 2021). As temperatures increase due to enhanced greenhouse gases, the air-column moisture content also increases, thus leading to an increase in convective available potential energy, representing a key ingredient favorable for the development of severe weather. In the current climate, hazards associated with severe storms

already threaten lives, infrastructure, and food and water supplies within the United States and elsewhere. With this in mind, an improved understanding of the causes and uncertainty of both near-term and longer-timescale variability in severe weather could aid in improving the accuracy of future predictions, as well as enhance resilience to severe weather outbreaks.

Due to their relatively small scale and intermittent occurrence, observing and collecting homogeneous records of severe weather events is difficult, especially when the weather events occur in relatively unpopulated or rural areas (Johns and Doswell 1992; Brooks et al. 2003). To partially offset the lack of direct, long-term, and reliable observations of severe storm events, the severe weather research community has developed convective indices and covariate proxies that represent the thermodynamic and kinematic components of the local storm environment and are indicative of conditions favorable for severe weather (Ludlam 1963; Rasmussen and Blanchard 1998; Craven and Brooks 2004). Consideration of these diagnostic variables can aid in determining the historical occurrence and future probability of severe weather, including the frequency, intensity, and type, or mode, of convection.

Convective Available Potential Energy (CAPE) is a measure of the potential energy available for upward vertical motion in a storm environment, whilst Convective Inhibition (CIN) is indicative of the boundary layer stability, which inhibits upward vertical motion. Considerable prior research has thoroughly investigated both the historical climatology as well as the projections of the future evolution of these parameters. In general, studies have shown that boreal spring CAPE is expected to increase substantially over the eastern continental U.S. (CONUS) by the end of the twenty-first century, largely as a result of an increase in specific humidity (e.g., Trapp et al. 2007; Trapp et al. 2009; Diffenbaugh et al. 2013; Seeley and Romps 2015; Hoogewind et al. 2017; Rasmussen et al. 2017; Chen et al. 2020; Lepore et al. 2021). Although less explored, the spatiotemporal evolution of boreal spring CIN is also in general agreement among previous studies, with increasing boundary layer stability by 2100, especially over the central CONUS (e.g., Hoogewind et al. 2017; Rasmussen et al. 2017; Chen et al. 2020; Lepore et al. 2021). While most of these studies have taken advantage of large-scale climate models to study changes in these convective indices, oth-

ers have taken a different approach by applying dynamical downscaling (Hoogewind et al. 2017; Chen et al. 2020). For example, Rasmussen et al. (2017) forced the regional Weather Research and Forecasting model (WRF, Powers et al. 2017) at 4 km resolution with ERA-Interim Reanalysis plus a climate change perturbation from a global climate model to investigate how CAPE, CIN, and their subsequent convective populations may change in the future. In particular, they calculated end-of-century monthly anomalies of CAPE and CIN relative to the historical climatology (1976-2005) using a 19-model CMIP5 ensemble mean under a strong, future emission scenario. Their results are broadly consistent with the aforementioned results, projecting increases in spring and summer CAPE and CIN over the eastern CONUS. Such findings suggest that in the future, weak to moderate storms will be less frequent because of increased stability, but the more intense storms will increase in frequency due to increased CAPE. In contrast, there is less agreement on projected end-of-century changes in tropospheric wind shear, which is a key factor for storm organization and severe weather. For instance, Trapp et al. (2007), Diffenbaugh et al. (2013), and Ting et al. (2019) used five different climate models with RCP8.5 forcing and found a robust swath of decreasing wind shear over most of the CONUS during the spring season, whilst Hoogewind et al. (2017) and Lepore et al. (2021) both found increasing wind shear over the western and central U.S. with decreasing shear over the eastern U.S. by 2100.

While changes in individual convective indices are useful for analyzing specific characteristics of storms, integrated measures of changes in storm environments, such as the product of CAPE and the wind shear between the surface and 6-km (S06), can provide a more complete description of the convective environment in time and space. By definition, CAPES06 considers both the thermodynamic energy and the kinematic motion in a storm environment. As a result, increases in this variable could signify an increase in the frequency of significant severe storms vs. non-severe storms (Rasmussen and Blanchard 1998; Brooks et al. 2003; Brooks 2009). On average, the historical climatology of warm-season CAPES06 produces a large-scale, spatially coherent pattern over the eastern CONUS, reflecting the climatology of the CAPE index (Brooks et al. 2003; Li et al. 2020). Simulations of future projections suggest a similar behavior for CAPES06, mirroring

the changes in CAPE. In particular, Seeley and Romps (2015) used a subset of climate models from phase 5 of the Coupled Model Intercomparison Project (CMIP5; Taylor et al. 2012), that were chosen based on their ability to reproduce a radiosonde climatology of severe storm environments, to compare twenty-first century changes in the frequency of environments favorable for severe weather using a CAPES06 threshold. In general, all four models produced changes for end-of-century CAPES06 that were of the same order of magnitude and showed consistent spatial patterns with increases over the southern and central U.S. ranging from 50 to 180% from the historical climatology (Seeley and Romps 2015).

Another approach has been to consider a combination of multiple convective indices to determine the number of days with severe weather environments (NDSEV, Brooks et al. 2003) for a particular time period or region. Previous studies agree that NDSEV will increase over much of the U.S. during the spring season, but differences exist in the projected magnitudes of the increases. For instance, Trapp et al. (2007, 2009) and Diffenbaugh et al. (2013) find an increase of ~ 3 days per season over the central and eastern CONUS by 2100, whereas Hoogewind et. al (2017) found an increase of ~ 10 days per season over the eastern CONUS by the end of this century. Such discrepancies are likely a consequence of varying definitions used for the NDSEV parameter, as well as model and emission scenario differences, and contrasting time periods of each of these studies. Hoogewind et al. (2017) also used dynamical downscaling to project end-of-century changes in the number of hazardous convective weather days (HCW), a proxy for when upward vertical velocity exceeds a certain threshold, as an indication of convective initiation. The projections of HCW were then used to correlate and compare to NDSEV values obtained from a climate model. The results illustrate that both severe weather proxies are expected to increase by 2100 and that the spatial patterns of change are highly correlated. This suggests that although NDSEV projections do not consider convective initiation and thus are likely to overestimate the number of days favorable for severe weather, it does well at estimating the important changes in the large-scale convective environment using both coarse grid climate models and convection-permitting regional models.

Until this point, the aforementioned studies have provided well-documented insight and have set the foundation for the types of changes that are likely to be experienced in future convective environments during the boreal spring. Primarily, they use either small sets of ensembles from a single model (<12), short integration periods($\sim$ 30 years), or multi-model ensemble means with different emission scenarios and other model variations to compare changes in convective environments due to anthropogenic forcing. Nevertheless, an additional and important perspective can be gained by utilizing a large-ensemble approach, whereby many simulations of the future are run under the same radiative forcing scenario but are started from slightly different initial conditions. The significance of this approach arises from the presence of unpredictable, internal (or natural) climate variability, which results in a range of possible future outcomes, all of which can be considered a possible reality (e.g., Deser et al. 2012b). Internal variability is one of the largest factors of unavoidable uncertainty in regional climate projections and can either enhance or suppress the forced signal (Deser 2020). It is important to note that each simulation in the ensemble contains a common response to the radiative forcing superimposed upon a different sequence of internal variability. In general, internal climate variability is larger in the extra-tropics than in the tropics and is relatively stronger compared to forced climate change when examining climate changes several decades into the future (Hawkins and Sutton, 2009; Deser et al. 2012b; Milinksi et al. 2020), as we will do in this project. A handful of studies have examined the relationship between severe weather and modes of climate variability such as the El Niño Southern Oscillation (e.g., Allen et al. 2015) and the Madden Julian Oscillation (e.g., Thompson and Roundy 2013). Each of these studies have found evidence suggesting a relationship between severe weather environments and various phases of these coupled interactions. For instance, Allen et al. (2015) found that fewer tornado and hail events occur over the central U.S. during El Niño events than during La Niña events. Thompson and Roundy (2013) showed that violent tornado outbreaks in the months March-May are more than two times as frequent during the second phase of the Real-time Multivariate MJO (RMM) index than during any other phases or during inactivity. These results are critical in helping to better understand the patterns of severe weather outbreaks as well as aiding in increasing the

skill for long-range seasonal predictions severe weather events (Allen et al. 2015). However, how low-frequency, unforced climate variability modulates the convective mode (i.e. frequency and storm type), as well as the thermodynamic and kinematic environment critical for severe weather, has not been examined extensively to date, even though it is likely a dominant influence regionally.

As such, this study hopes to build on the previous literature, specifically by taking advantage of a newly released large-ensemble of simulations from the Community Earth System Model (CESM) Version 2.0 (Danabasoglu et al. 2020), hereafter referred to as the CESM2-LE (Rodgers et al. 2021). Leveraging the CESM2-LE, which extends from 1870-2100, allows us to evaluate the temporal evolution of convective environments over a much longer, continuous-time record than has been done before. Further, it allows us to robustly examine both the forced variability due to anthropogenic climate change, as well as the possible role of internal variability in modulating the forced signal over the coming decades. To our knowledge, these aspects related to severe weather environments in the U.S. have yet to be rigorously examined, and thus represent a novel aspect of the current study. An increased understanding of the possible combined effects of forced and internal variability on convective environments is important for ensuring that climate adaptation policies are based on the most complete, scientific information available (Deser 2020; Mankin et al. 2020).

Chapter 2

Methodology

We utilize simulation data from the CESM (Hurrell et al. 2013). The open-source CESM is unique in that it is both developed and applied to scientific problems by a large community of researchers. It is a critical infrastructure for the U.S. climate research community and is principally funded by the National Science Foundation (NSF) and managed by the U.S. National Center for Atmospheric Research (NCAR). Simulations performed with the CESM have made many significant contributions to climate research, ranging from paleoclimate applications (e.g., Otto-Bliesner et al. 2016) to contributions to the North American Multi-Model Ensemble (NMME, Kirtman et al. 2014) seasonal forecasting effort led by the National Oceanic and Atmospheric Administration (NOAA). Simulations with CESM have also been used extensively in both national and international assessments of climate science, including substantial contributions to version 6 of the CMIP (CMIP6; Eyring et al. 2016). The salient point is that CESM provides the broader academic community with a core modeling system to investigate a diverse set of earth system interactions across multiple time and space scales.

2.1 Model Information and Data

Daily data for specific humidity, column air temperature, near-surface (10-meter) wind speed, zonal and meridional winds, and geopotential heights were obtained from a recent large-ensemble produced with CESM2. The CESM2-LE uses the Community Atmosphere Model version 6 (CAM6), which is a 'low-top' model consisting of 32 vertical levels (a relatively coarse stratospheric representation) and a nominal 1° (1.25° in longitude and 0.9° in latitude) spatial resolution. To study the temporal evolution of the severe weather environment over the CONUS during boreal spring (March-June), 50 ensemble members were analyzed spanning 1870-2100. Each ensemble member used CMIP6 forcings over the historical record and a future (2015-2100) forcing of SSP3-7.0 (Rodgers et al. 2021), a medium-high emissions scenario resulting in approximately 7.0

W/m^2 in radiative forcing by the end of the twenty-first century (O'Neill et al. 2016; IPCC 2021). This level of forcing is a policy-relevant target, and it is a more moderate forcing scenario than those analyzed in most previous studies that have examined future changes in convective indices. An ensemble of this size and duration with a CMIP6 generation Earth system model provides an unprecedented opportunity to investigate the long-term evolution of the large-scale convective environments, how it is impacted by forced variability, and to what extent the latter is influenced by internal climate variability.

2.2 Relevant Parameters

The CESM2-LE simulations were used to compute several parameters to help quantify the thermodynamic and kinematic characteristics of the large-scale storm environment across the U.S. CAPE (Jkg^{-1}) has historically been known as a quantity most closely associated with the potential occurrence of deep convection (Doswell III and Rasmussen 1994; Riemann-Campe 2009). This thermodynamic parameter is formally defined as the vertical integral of buoyancy from the level of free convection to the equilibrium level, making it suitable to diagnose conditional instability and potential updraft strength (Holton 1972). We have chosen to use the most-unstable CAPE in the lowest 300-mb to ensure that our analysis captures any potentially elevated convection, as well as the maximum instability (Rochette et al. 1999). CAPE was calculated using the equation below, where R$_d$ is the ideal gas constant, p$_{EL}$ and p$_{LFC}$ are the pressures at the equilibrium level and the level of free convection (LFC), and T$_{vp}$ and T$_{ve}$ are the virtual temperatures of the parcel and the environment, respectively.

$$\mathbf{CAPE} = \mathbf{R_d} \int_{\mathbf{p_{LFC}}}^{\mathbf{p_{EL}}} (\mathbf{T_{vp}} - \mathbf{T_{ve}}) \mathbf{d ln(p)} \tag{2.1}$$

CIN (Jkg^{-1}) is equal to the negative buoyancy, or the negative work done by the atmospheric boundary layer as a parcel ascends from the surface through the stable layer to the LFC (Colby 1984; Rasmussen and Blanchard 1998; Riemann-Campe 2009). It is routinely analyzed to evaluate the stability of the local atmosphere and the potential suppression of convective motions. As CIN is the amount of energy an air parcel needs to overcome in order to reach the LFC, we will hereafter define it as a negative value (i.e., more negative values mean more convective inhibition). The equation for this parameter is listed below, where p_{SFC} is the pressure at the surface.

$$\mathbf{CIN} = \mathbf{R_d} \int_{\mathbf{p_{SFC}}}^{\mathbf{p_{LFC}}} (\mathbf{T_{vp}} - \mathbf{T_{ve}}) \mathbf{d ln(p)} \tag{2.2}$$

To explore the kinematic components of the convective environment, we used the difference in the bulk vertical wind shear from 10 meters above ground level ($\sim$ 925-mb) to 6-km ($\sim$ 525-mb) above ground level, known as S06 (ms^{-1}). Past work suggests that while lower-level wind shear is important for tornadic environments, S06 is one of the best indices for determining storm type and organization (Rasmussen and Blanchard 1998; Weisman and Rotunno 2000; Brooks et al. 2003). Large values of S06 are characterized by thunderstorms with stronger mid-level rotation. Such storms have increased organization for storm dynamics such as a tilted updraft, which is necessary to displace the area of upward vertical motion from the downward vertical motion. This increases storm longevity, as well as the potential for the storm to form a mesocyclone and develop into a supercell, which is typically accompanied by severe weather hazards.

$$\mathbf{S06} = (\mathbf{V_{6-km}} - \mathbf{V_{10-m}}) \tag{2.3}$$

We also compute a covariate convective index, which is the product of CAPE and S06, or CAPES06 (m^{3}s^{-3}). Previous research has demonstrated the effectiveness of using CAPES06 to help discriminate between significant severe storms and less severe events (Rasmussen and Blanchard 1998; Craven et al. 2002; Brooks et al. 2003; Brooks 2009; Seeley and Romps 2015). CAPES06 takes into account two of the most necessary components for convection: the ther-

modynamic energy and the kinematic structure. High values of this parameter are indicative of increased storm organization and higher updraft velocities. Historically, soundings from days with the most severe storms exhibited high values in this parameter (e.g., Rasmussen and Blanchard 1998; Brooks et al. 2003; Brooks 2009).

$$\mathbf{CAPES06} = \mathbf{CAPE} * \mathbf{S06} \tag{2.4}$$

Finally, to convey the integrated effects of all of these convective indices, we also examine changes in NDSEV. Following the definition used in past studies (Brooks et al. 2003; Trapp et al. 2007; Gensini and Ashley 2011; Hoogewind et al. 2017), a day is counted as a severe weather day when CAPE $\geq$ 100 Jkg^{-1}, CIN $\geq$ -100 Jkg^{-1}, S06 $\geq$ 5 ms^{-1}, and CAPES06 $\geq$ 10,000 m^{3}s^{-3}. We then sum the number of days that meet these criteria throughout the boreal spring season of obtain an estimate of the potential number of severe weather days.

This study will focus primarily on the eastern CONUS region outlined in Figure 2.1, which is a highly active region for intense convection. Note, however, that ocean regions are masked from our analysis, so that we are focusing on convective indices over land only. We define the spring season as March through June (MAMJ), as this period captures the months when storms are most frequent and violent over the eastern CONUS (Kelly et al. 1985; Brooks et al. 2003; Gensini and Ashley 2011; Li et al. 2020). Later into the summer season, the temperature and moisture gradients in this region are weaker, and the jetstream begins to shift north away from the main source of energy, resulting in an overall northward shift in convective activity.

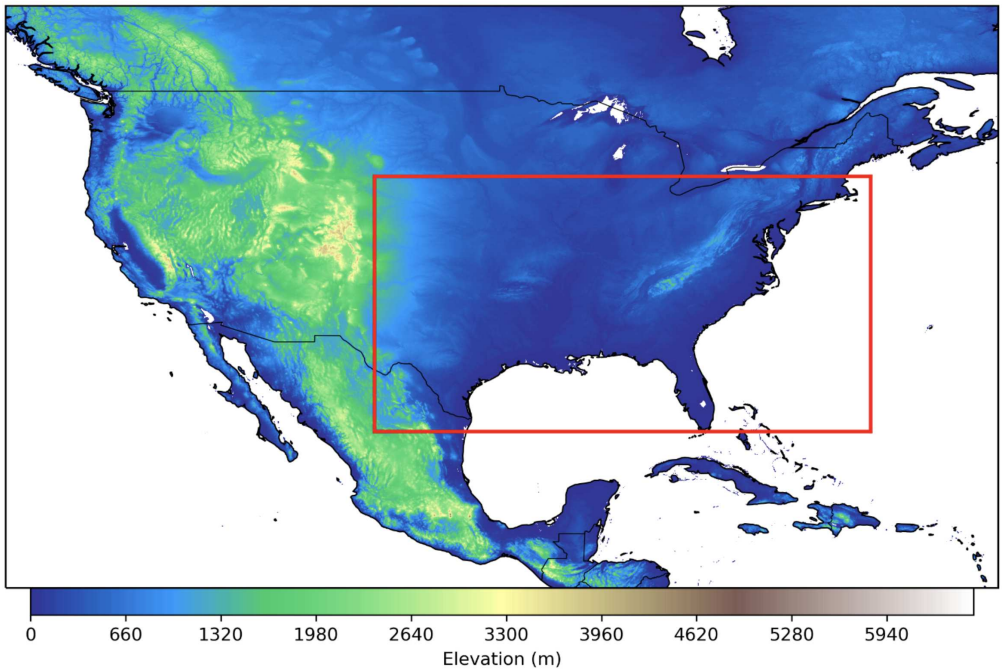

Figure 2.1: Southeast CONUS domain used for this study. Latitude bounds are between (25°N and 43°N) and longitude bounds are between (-104°W, -69°W).

2.3 Model Verification

To verify that the CESM2-LE is a viable tool for our analysis, the fifth-generation global climate reanalysis (ERA5, Hersbach et al. 2020) from the European Centre for Medium-Range Forecast (ECMWF) was used for model validation. Previous studies have found ERA5 to be reliable in capturing the spatiotemporal climatology of convective environments (Taszarek et al. 2021). Li et al. (2020) conducted a climatological analysis of severe local storm environments over North America using ERA5 compared to CAM6 simulations of the historical period. They confirmed the validity of ERA5 against 69 radiosonde observations over the CONUS region with twice daily raw soundings and further confirmed the fidelity of CAM6 against ERA5. This is important because, since its predecessor CAM5 (Neale et al. 2012), CAM6 underwent significant modifications to the physical parameterization suite. For instance, updates to the Zhang and McFarlane (1995) deep convection and orographic drag parameterizations were implemented into CAM6, along with the two-moment prognostic cloud microphysics from Gettelman and Morrison (2015). Additionally,

the Cloud Layers Unified by Binormals (CLUBB, Golaz et al. 2002) replaced schemes for cloud macrophysics, boundary layer turbulence, and shallow convection previously used in CAM5, all of which are key parameterizations for modeling convection.

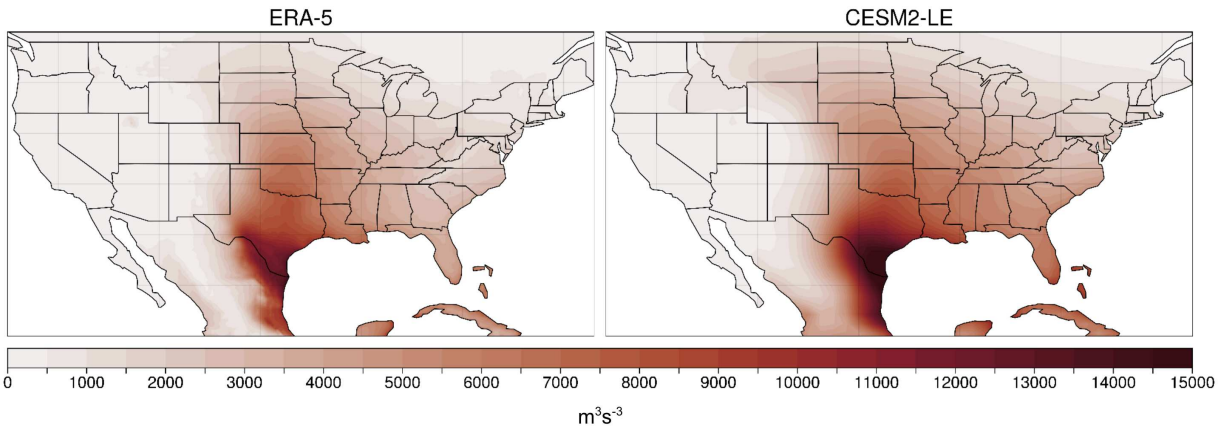

Figure 2.2: MAMJ CAPES06 (m^3s^{-3}) climatology for ERA5 reanalysis (left) and the CESM2-LE ensemble-mean (right) for the 1980-2019 period.

Figure 2.2 shows the MAMJ CAPES06 climatology from ERA5 and the ensemble-mean climatology from CESM2-LE over the CONUS region. There is strong agreement between the CESM2-LE and ERA5 during 1980-2019, indicating that the model successfully captures the mean spatial characteristics of CAPES06 over the past 40 years due to anthropogenic climate change. Similarly strong agreement is found between ERA5 and CESM2-LE for the climatologies of the other convective indices (CAPE, CIN, and S06 - not shown).

To further examine the fidelity of the CESM2-LE, we investigated the relationship between CAPES06 and the El Niño Southern Oscillation (ENSO) phenomenon, the largest driver of interannual changes in weather and climate over much of the globe (Ropelewski and Halpert 1986; Dai et al., 1997; Allen et al. 2015; Dai and Wigley 2000). Figure 2.3 illustrates the regression from ERA5 onto the observed Niño3.4 index over 1980-2019 during the spring season, compared to the same quantity from the CESM2-LE over 1870-2019. Notably, CESM2-LE captures the main changes in CAPES06 associated with ENSO, including large-scale decreases in CAPES06 over the eastern CONUS during El Niño, with increases over the western CONUS. Since we are using

a large-ensemble, many more El Niño events are sampled from the CESM2-LE data than from ERA5, resulting in more coherent spatial patterns. This relationship is consistent with other studies that have investigated the role of ENSO on severe weather outbreaks over the U.S. during the March-May season (e.g. Lee et al. 2013; Allen et al. 2015). The results in this section, combined with the findings of earlier studies (e.g., Li et al. 2020), give us confidence in using the CESM2-LE to examine past and future changes in convective environments over the CONUS, as well as the variations driven by internal modes of climate variability (e.g., Capotondi et al. 2020; Rodgers et al. 2021).

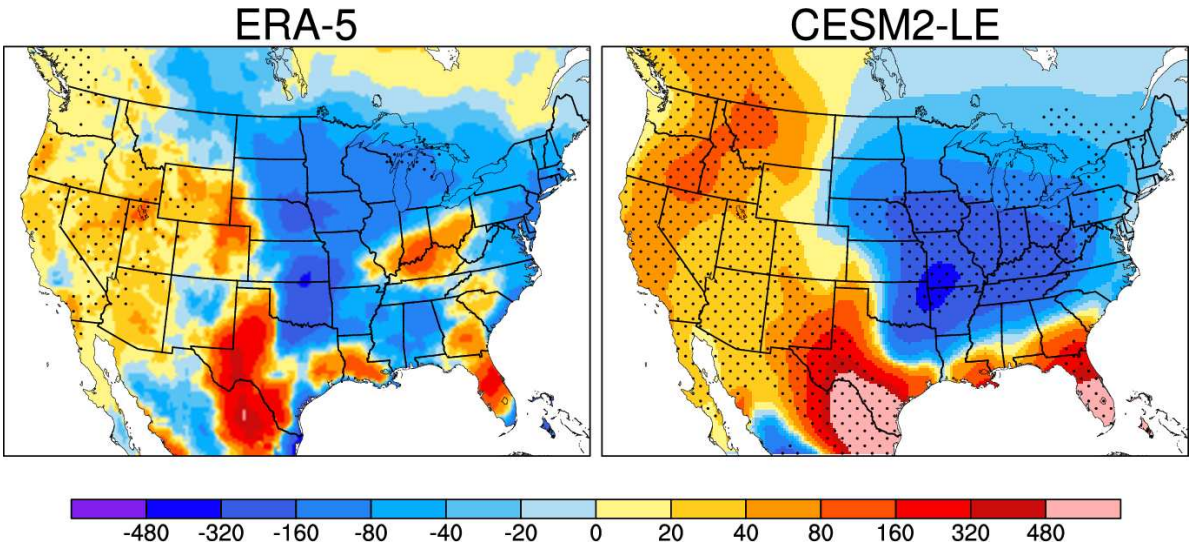

Figure 2.3: Regression of CAPES06 onto the ENSO index for one standard deviation over the 1980-2019 MAMJ season from ERA-5 reanalysis (left) and the CESM2-LE (right). Stippling on ERA-5 (left) shows the 95% statistical significance based on the Students T-test. Stippling on CESM2-LE (right) indicates where 45 of the 50 members have the same sign.

Chapter 3

Results

3.1 Ensemble Mean (Forced Changes)

We begin by evaluating the historical and future time evolution of the selected convective indices from 1870-2100 for the boreal spring season (March-June) averaged over the eastern CONUS (Figure 2.1). Time series are expressed as anomalies relative to the 30-year base period 1971-2000 (Figure 3.1). The forced component of climate change is given by the ensemble-mean of the CESM2-LE, represented by the solid black line, while the time histories of individual ensemble members are depicted by light grey lines. While considerable run-to-run, interannual and decadal variability is evident in individual ensemble members, the forced changes in convective indices show little change from 1870 until about 1990, deviating little from the 30-year climatologies until just prior to the year 2000. Thereafter, forced changes in convective environments, due to anthropogenic climate change, become apparent and exhibit clear departures from the historical climatological values throughout the century. For instance, ensemble-mean values of CAPE steadily increase throughout the twenty-first century, exceeding the historical climatological values by nearly 400 Jkg^{-1} by 2100 (Figure 3.1a), while the forced change in S06 becomes more negative. Specifically, anomalies in S06 reach $\sim$ 2 ms^{-1} by 2075, then remain at approximately that level until 2100 (Figure 3.1b).

The time evolution of CAPES06 (Figure 3.1c) exhibits behavior similar to that of CAPE, with an almost linear increase of $\sim$ 3500 m^3s^{-3} above the climatology by 2100. The time history of CIN also shows little deviation until this century, when it exhibits a steady decrease to approximately -18 Jkg^{-1} by 2100 (Figure 3.1d). These results show that changes in convective environments due to anthropogenic forcing through the end of this century are prominent and robust in CESM2-LE, as they are reflected in nearly all of the 50 members of the ensemble (light grey lines in Figure 3.1). Few previous studies have examined the continuous-time evolution of changes in convective in-

dices, as is shown in Figure 3.1. One example is Diffenbaugh et al. (2013), who leveraged the CMIP5 to take regional averages over eastern CONUS for CAPE, S06, and NDSEV from 1960-2100 using RCP8.5. Furthermore, Trapp et al. (2009) used a five-member ensemble from the Community Climate System Model (CCSM3) to take regional averages over various CONUS regions that frequently encounter severe weather, including the southeast, Midwest, and the southern and northern Great Plains. This was done for the same indices as Diffenbaugh et al. (2013), except from 1950-2100. In general, the trends and magnitudes of the changes in these indices were in agreement with the changes expressed in Figure 3.1, especially over the southern Plains and southeast CONUS, as seen in Trapp et al. (2009). The principal point is that convective environments over the eastern CONUS during the boreal spring are likely to undergo substantial departures from the historical record (Figure 3.1), moving toward higher convective energy, more stability, and less kinematic support for the production of hazards associated with severe weather.

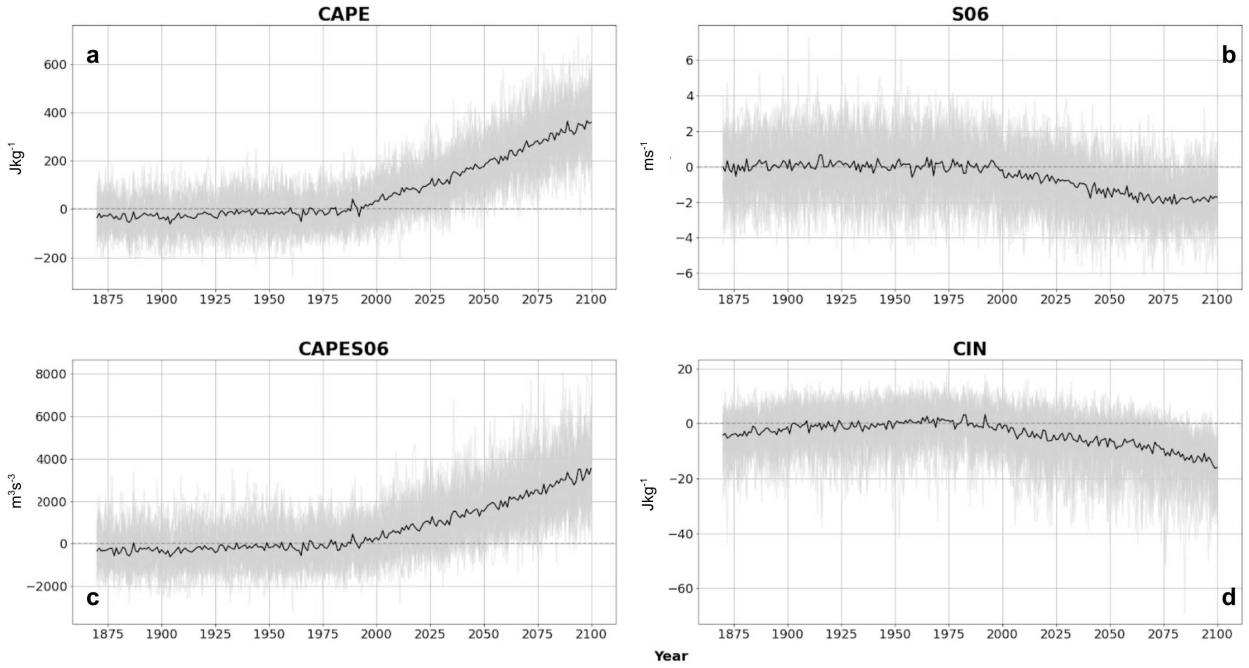

Figure 3.1: Time series of convective indices from 1870-2100 for (a) CAPE (Jkg^{-1}), (b) S06 (ms^{-1}), (c) CAPES06 (m^3s^{-3}), and (d) CIN (Jkg^{-1}) over the eastern CONUS region. The 50-member ensemble-mean (black) is superimposed on individual members (light grey).

To evaluate the spatial character of these changes over the CONUS, epoch differences for future 30-year periods relative to the 1971-2000 baseline climatology are shown in Figure 3.2. By 2100, the CESM2-LE projects spatially coherent forced changes in convective environments relevant to the frequency and intensity of severe weather over the CONUS. Over the next few decades (2021-2050), increases in CAPE are largest near the Gulf coast and are positive across the entire CONUS (Figure 3.2a). These changes in CAPE are projected to strengthen throughout the rest of this century, primarily over the eastern CONUS and southern Plains. As CAPE is related to the maximum potential updraft within a thunderstorm by $w_{max} = \sqrt{2 \times CAPE}$ (Holton, 1972), projections of higher CAPE imply that on average, future storms will have stronger updrafts, resulting in deeper, more explosive convection than storms during the reference period (1971-2000). The spatial patterns in these changes also highlight the continued influence of the GPLLJ advecting warm, moist air into the Plains and east of the Rocky Mountains (e.g., Carlson et al. 1983). This index is the most studied of the convective indices analyzed here, and our results are consistent with previous studies (Trapp et al. 2007; Diffenbaugh et al. 2013; Seeley and Romps 2015; Hoogewind et al. 2017; Rasmussen et al. 2017; Chen et al. 2020; Lepore et al. 2021).

Epoch differences in boreal spring wind shear reveal a large and spatially coherent east-west swath of decreasing S06 over the entirety of the CONUS, increasing in magnitude with time (Figure 3.2b). The greatest changes appear in the northeast, with smaller decreases over the southern CONUS. This finding is also consistent, both in magnitude and spatial extent, with the handful of previous studies that have analyzed end-of-century projections in vertical wind shear and found a robust decrease (Trapp et al. 2007; Diffenbaugh et al. 2013; Ting et al. 2019), rather than a bifurcation of S06 changes over the CONUS (Hoogewind et al. 2017; Lepore et al. 2021).

Sufficient shear is imperative to the internal dynamics of a thunderstorm since it promotes vertical storm-scale rotation and assists in sustaining the updraft (Weismann and Rotunno 2000; Trapp et al. 2007), which are important ingredients for tornadogenesis, large hail formation, and damaging outflow winds at the surface. Additionally, storm environments characterized by strong vertical wind shear are more likely to be organized, last longer, and become self-sustaining (e.g.,

Lilly 1979; Rotunno 1981; Klemp 1987; Weismann and Rotunno 2000). For these reasons, decreases in shear with time indicate that increasingly fewer thunderstorms will have the support necessary for the most hazardous and severe storms to form, including organized mesoscale convective systems (MCS).

To further diagnose the projected changes in S06, we examined the changes of zonal and meridional winds near the surface and at 6-km. Future projections of surface winds do not reveal coherent changes over the next century, but the zonal winds aloft indicate substantial departures from the historical record (Figure A.1, Figure A.2, and Figure A.3). In particular, nearly all of the CESM2-LE ensemble members project decreases in upper-level westerly winds over the CONUS during the boreal spring season that increase in magnitude with time. Further exploration into this response is needed to explain the causal mechanisms of these zonal wind changes, but preliminary results suggest a connection to projected changes in tropical rainfall (not shown). The key point is that decreasing westerlies aloft (i.e., anomalous easterlies) would inhibit the formation of strong mesocyclones, thus reducing the support and potential for the most severe weather. We note that these results are consistent with prior studies projecting an end-of-century decrease in boreal spring and summer wind shear over much of the CONUS, particularly eastern CONUS (Trapp et al. 2007; Trapp et al. 2009; Diffenbaugh et al. 2013; Hoogewind et al. 2017; Lepore et al. 2021; Ting et al. 2019).

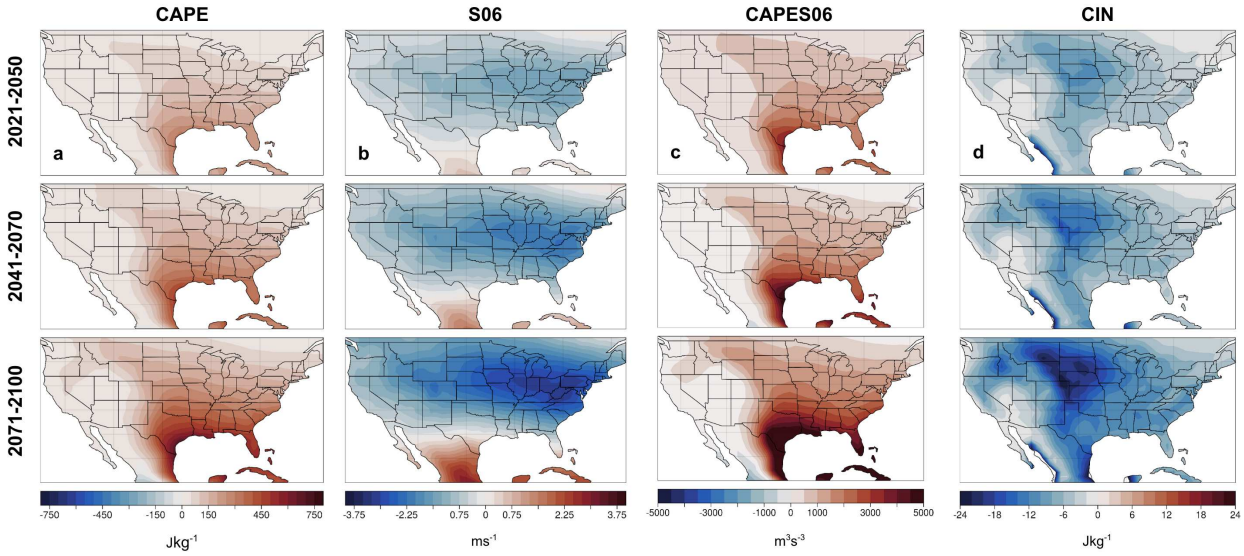

Figure 3.2: Epoch differences from the 1971-2000 baseline period for early (2021-2050), mid (2041-2070), and end-of-century (2071-2100) convective indices during MAMJ for (a) CAPE (Jkg^{-1}) (b) S06 (ms^{-1}) (c) CAPES06 ($\mathrm{m}^3\mathrm{s}^{-3}$) and (d) CIN ($\mathrm{Jkg}^{-1}$)

The projected spatial characteristics of changes in CAPES06 (Figure 3.2c) are similar to those highlighted by Seeley and Romps (2015), who leveraged four climate models, archived from CMIP5 and forced with two different emission scenarios, to compare the end-of-century projections of CAPE $\times$ S06 over the U.S. Overall, their findings, as well as ours, show spatial patterns of boreal spring CAPES06 that mirror changes in CAPE (Figure 3.2a), characterized by a coherent increase with time over the eastern CONUS. The index CAPES06 has historically been used to distinguish between severe and non-severe storms, as it considers both thermodynamic and kinematic components of a thunderstorm. Although decreases in S06 suggest that there would be less support for storm organization and dynamics, some studies speculate that the large-scale increases in CAPE will make up for the diminishing S06 (e.g., Trapp et al. 2007; Trapp et al. 2009), but to our knowledge, this has yet to be extensively examined and remains a subject of future work. The main point is that CAPES06 is expected to undergo substantial increases by the end of this century, suggesting convective environments over the southeastern U.S. will be supportive of a higher ratio of significant severe versus non-severe storms.

Changes in the forced component of CIN projected by the CESM2-LE are characterized by decreases over the central and northern Great Plains that increase in magnitude throughout this century, reaching approximately -18 Jkg^{-1} by 2100 (Figure 3.2d). Such changes are indicative of a more stable or "capped" atmosphere. If strong enough (CIN < -200 Jkg^{-1}), this stability could potentially inhibit convection completely. On the other hand, there is the possibility that there is moderate CIN (-50 Jkg^{-1} > CIN > -200 Jkg^{-1}), allowing for an accumulation of CAPE that once released, could produce explosive convection. Globally, this is commonly observed in convective environments in the vicinity of large mountain ranges such as the Rockies and the Andes, as discussed in the introduction. The juxtaposition of the terrain-induced mid-level capping inversion with the warm, moist air allows for the modulation of CAPE by CIN until convective initiation occurs and develops explosive convection. It is also evident in spatial patterns (Figure 3.2) that the areas of average maximum stability are not colocated with the areas of average maximum convective energy. Therefore, since CIN is minimized over the Great Plains, while CAPE is maximized over the eastern U.S., the future frequency of convection in the Great Plains is, on average, likely to be less than the current climate but still strong, while convective frequency over the eastern U.S. is likely to be slightly less reduced, but more explosive when it does occur. Overall, these changes are in general agreement with previous studies using global climate models (Hoogewind et al. 2017; Lepore et al. 2021), as well as with studies that have used dynamically downscaled high-resolution regional models, such as Rasmussen et al. (2017) and Chen et al. (2020), projecting coherent decreases in CIN over the central and southern Great Plains by 2100 (Figure 3.2d).

Following the analyses of Brooks et al. (2003), Trapp et al. (2007), and Gensini and Ashley (2011), we identify the number of days favorable for the formation of severe weather during the four-month boreal spring season by computing NDSEV. Early-century (2021-2050) changes from the baseline climatology show an increase in boreal spring NDSEV that is especially pronounced over the eastern half of the CONUS, with the largest values over the southeastern U.S. (Figure 3.3; top). Increases in NDSEV continue throughout the rest of this century (2041-2070), yielding values more than double the historical climatology, and largely reflecting spatial patterns evident in

CAPE (Figure 3.2a). These findings are further evidence that by 2100, eastern CONUS will likely experience an increase in severe storm activity (Figure 3.3; bottom), despite the robust decrease in projections of S06, especially since the end-of-century magnitudes are still larger than the severe weather threshold (5 ms^{-1}). Moreover, since the greatest increases in CAPE are shown to correspond with small, but spatially robust, decreases in S06, there is a net increase in the NDSEV due to an average increase in CAPE (Diffenbaugh et al. 2013). The spatial patterns of change in NDSEV are in broad agreement with previous results that analyze similar regions and time periods (Trapp et al. 2007; Trapp et al. 2009; Diffenbaugh et al. 2013; Hoogewind et al. 2017), although, the magnitude of changes expected by the end of the century are almost 3 times larger than the aforementioned studies. A detailed explanation for these differences is beyond the scope of this paper, but it is important to note that other studies used slightly different definitions of NDSEV, as well as different models and forcing scenarios, all of which likely contribute to the discrepancies from the results shown here in Figure 3.3.

As expressed, the findings presented in this section are all in good agreement with previous literature. What makes this work unique is that we have been able to show a robust estimate of the large-scale convective environments by using a 50-member ensemble from the CESM2 giving us more certainty in the changes of the forced response due to anthropogenic climate change. Although, uncertainty in the forced response also arises from the influence of internal variability from one run to the next, which we will attempt to qualitatively analyze and investigate in more detail in the next section.

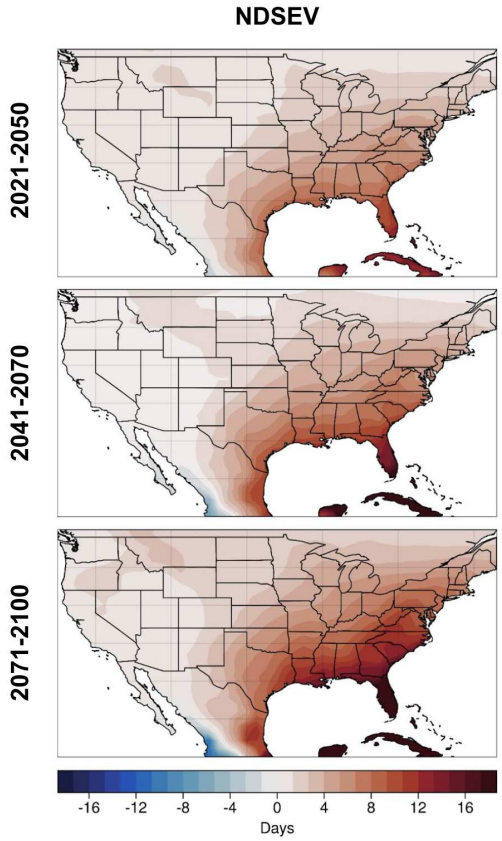

Figure 3.3: Same as Figure 3.2, except for NDSEV (DaysDecade^{-1}).

3.2 Internal Variability

Thus far, the aforementioned studies have primarily focused on changes in convective environments due to the forced response, or anthropogenic climate change. However, the large-ensemble approach presents the novel opportunity to investigate the effect of internal (or unforced) climate variability and how it might modify the forced response, where all 50 ensemble members represent an equally possible path to reality. By taking the mean of all the members, we can decompose a single simulation to isolate the forced and internal variability of the climate system.

To illustrate the range of possible outcomes, we consider the simple metric of linear trends in each of the convective indices over the next 30 years (2021-2050). Histograms of these are shown in Figure 3.4. Changes through 2050 are analyzed simply because uncertainty due to internal climate variability is most significant over the next several decades relative to the forced signal (Hawkins and Sutton 2009; Deser 2020).

Even in the presence of significant internal variability, 30-year trends of boreal spring CAPE over the eastern CONUS are positive for all 50 ensemble members (Figure 3.4a), but they exhibit considerable spread. Extreme trends range from near zero to $\sim$ 68 Jkg^{-1}Decade^{-1}, while two-thirds of the ensemble members have CAPE trends between 20 and 40 Jkg^{-1}Decade^{-1}. Similarly, trends in S06 are mostly of the same sign, with 46 of the 50 ensemble members exhibiting negative trends with a minimum of approximately -0.85 ms^{-1}Decade^{-1} projected by four members. These results show that the sign of the response of CAPE and S06 to anthropogenic forcing (Figure 3.1a, b) is robust across nearly all of the CESM2-LE members, but that the forced response is likely to be considerably moderated by internal climate variability over the coming decades (Figure 3.4a, b).

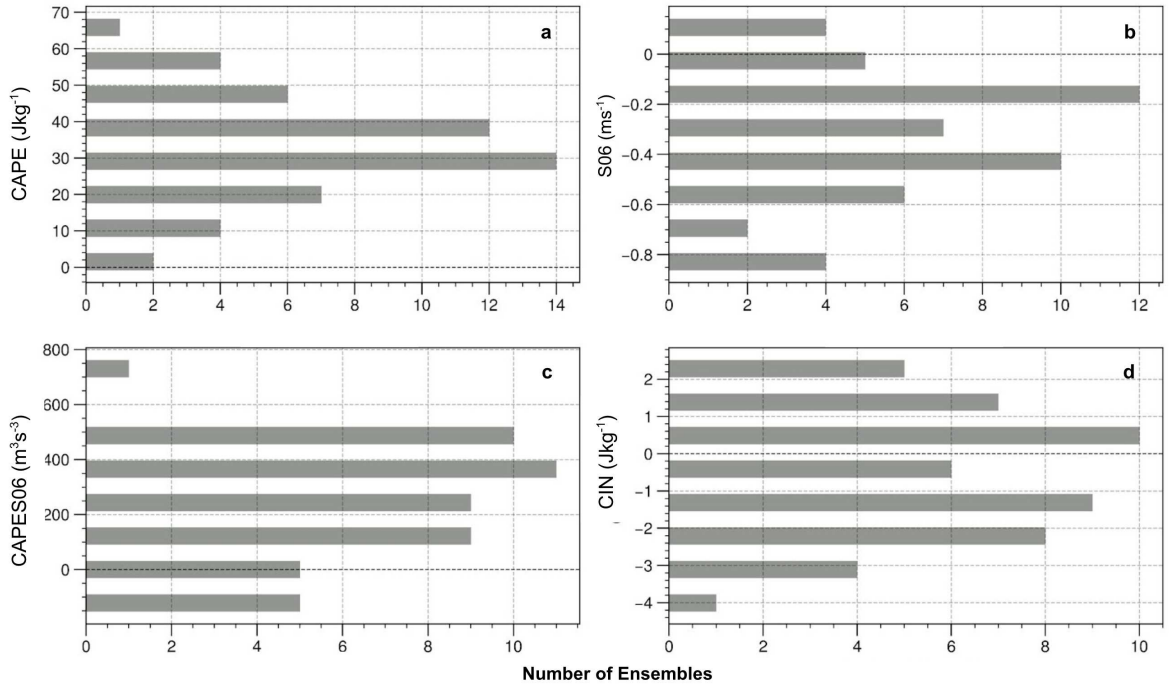

Figure 3.4: Histograms for 50-member ensemble simulations illustrating the spread of linear trends per decade for the 2021-2050 period during the months March - June for (a) CAPE ($Jkg^{-1}Decade^{-1}$) (b) S06 ($ms^{-1}Decade^{-1}$) (c) CAPES06 ($m^3s^{-3}Decade^{-1}$) (d) CIN ($Jkg^{-1}Decade^{-1}$). Linear trends were calculated using a 3rd-degree polynomial fit and spatial averages were taken over the eastern CONUS region highlighted in Fig. 1.

Moreover, boreal spring trends in CAPES06 over the coming decades are positive for nearly all ensemble members (Figure 3.4c), with 80% of the members exhibiting trends between 100 and 500 $m^3s^{-3}Decade^{-1}$. In contrast, the sign of 30-year trends in boreal spring CIN over the eastern CONUS are more bifurcated (Figure 3.4d). Twenty-one of the ensemble members exhibit positive trends, while the other 29 exhibit negative trends down to -4.25 $Jkg^{-1}Decade^{-1}$ (Figure 3.4d). While Figure 3.1d and Figure 3.2d illustrates a forced decrease in CIN magnitudes by the end of the century, the robustness of the sign of the change is less certain due to the influence of internal climate variability (Figure 3.4d).

To further express the dominant role that internal variability is likely to play over the next several decades, we examine spatial patterns of change by selecting the ensemble members with the largest and smallest trends in area-averaged CAPES06 over the eastern CONUS during the boreal spring (Figure 3.5) from the histograms shown in Figure 3.4. CAPES06 is shown since it considers two of the most important elements necessary for severe weather: thermodynamic energy and kinematic support.

Ensemble-member 25 exhibits the most negative (minimum) trend (-182 $Jkg^{-1}Decade^{-1}$) when averaged over the eastern CONUS, while ensemble-member 23 has the largest trend (791 Jkg^{-1}-$Decade^{-1}$). The spatial patterns of the linear trends in CAPES06 for these two simulations are shown in Figure 3.5a and Figure 3.5d, respectively. By removing the forced (ensemble-mean) trend from each of these individual ensemble members (Figure 3.5b ,e), the changes in CAPES06 over the next several decades due purely to internal variability are revealed (Figure 3.5c ,f). In general, the signals of internal climate variability are spatially coherent and are of a larger magnitude over the next several decades than the forced trends. In ensemble-member 25, internal climate variability counteracts the forced, positive change in CAPES06 over much of the southeastern U.S (Figure 3.5c), resulting in an overall negative trend over much of the region (Figure 3.5a). Conversely, in ensemble-member 23, internal climate variability augments the forced signal (Figure 3.5d) and produces a very strong increase through 2050, especially over parts of Texas and the southern Great Plains (Figure 3.5f). These two ensemble members were subjectively selected to most dramatically illustrate the role of internal climate variability in modulating the forced response in CAPES06, but a similar approach can be taken with the other ensemble members in Figure 3.4 to illustrate the spatial patterns of internal variability. In other words, the spatial pattern of forced change in CAPES06 is likely to be significantly modified by internal climate variability, as is the case for other climate variables such as surface temperature, pressure, and precipitation (Deser 2020).

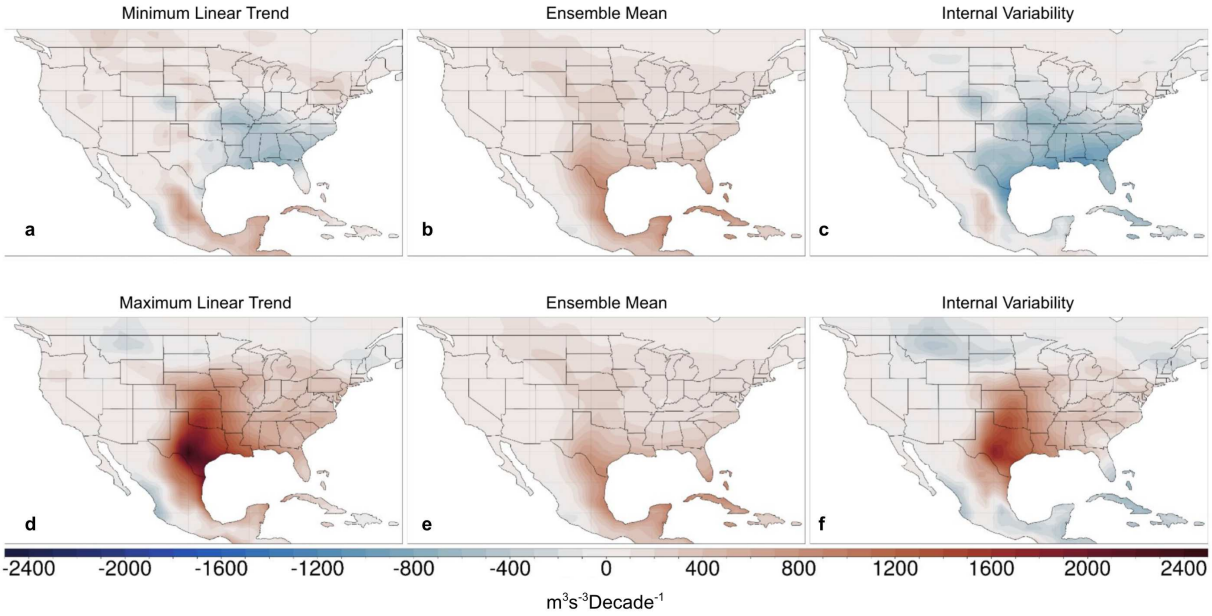

Figure 3.5: Linear decadal trends for 2021-2050 over the eastern U.S. for the ensemble numbers 25 (top) and 23 (bottom) for the full (left), forced (middle), and internal (right) components of MAMJ CAPES06 ($m^3s^{-3}Decade^{-1}$).

Similarly, in Figure 3.6 we illustrate the dominant role of internal variability in affecting NDSEV. Over the next several decades (2021-2050), anthropogenic climate change is likely to increase the number of days in boreal spring with convective environments favorable for the development of severe weather over most of the CONUS, with the largest increases over the southeastern U.S. (Figure 3.6b, Figure 3.6e). However, as shown by ensemble-member 41 (Figure 3.6a), a plausible outcome by 2050 is that internal climate variability could substantially reduce the number of days favorable for severe weather (Figure 3.6c). Conversely, ensemble-member 23 shows that internal climate variability might augment the increases from climate change (Figure 3.6f), resulting in an extreme increase in decadal trends of NDSEV (Figure 3.6d), as was seen with CAPES06 and other convective indices (not shown).

Such internally-driven variations have substantial magnitudes and also show significant spatial coherency. While the internal fluctuations may be considered to be inherently chaotic and random, they are a product of the large-scale dynamics and have proven to be spatially coherent with rela-

tively large magnitudes (Figure 3.5c, f and Figure 3.6c, f). However, the circulation anomalies that drive such internal variations in these convective parameters are the subject of future work. The key point is that internal variability is likely to either significantly dampen or enhance the response of convective environments to anthropogenic forcing. Therefore, as there is no way to accurately predict which will occur, it becomes crucial that when making future projections we not only consider what the forced response will be, but the extent to which it will be modulated by internal variability.

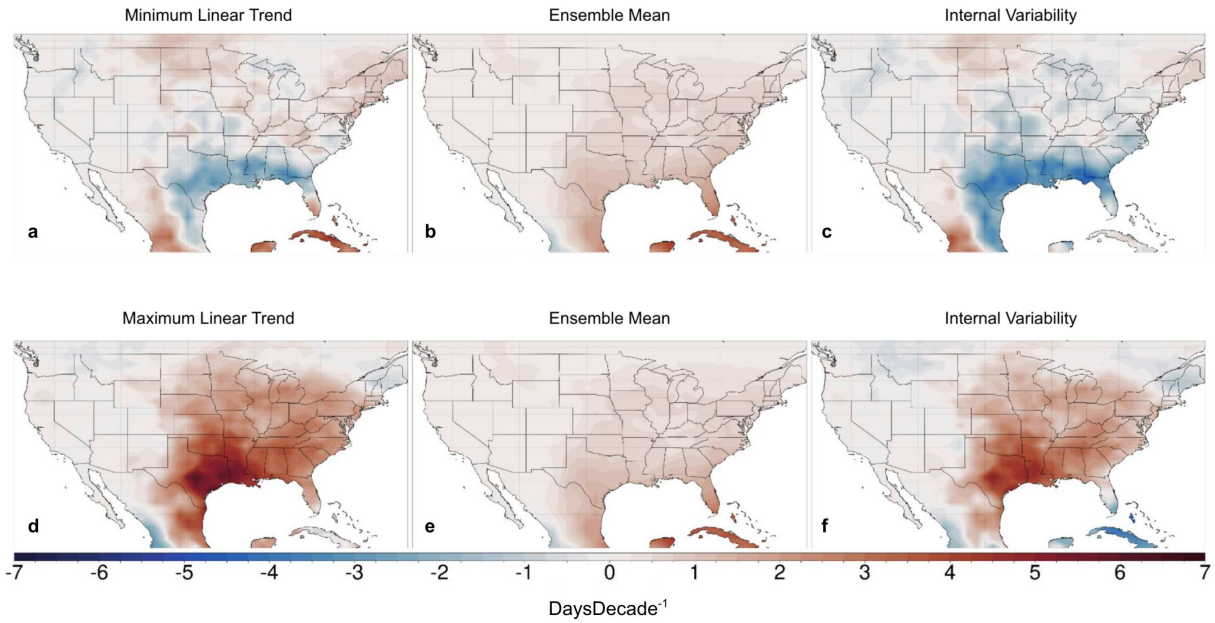

Figure 3.6: Linear decadal trends for 2021-2050 over the eastern U.S. for the ensemble numbers 41 (top) and 23 (bottom) for the full (left), forced (middle), and internal (right) components of MAMJ NDSEV (DaysDecade^{-1}).

In addition to employing covariate proxies, epoch bivariate distribution plots, or two-dimensional histograms, were created to examine the future phase spaces (i.e. convective frequency and intensity) of various convective indices, due to both forced and internal variability, to gain more insight into the changes in convective mode, frequency, and intensity. As mentioned, Rasmussen et. al (2017) used dynamical downscaling to produce convection-permitting regional climate model projections of end-of-century (2071-2100) May-June CAPE and CIN over the Midwest to exam-

ine changes in the thermodynamic environment. By producing a two-dimensional histogram, they found that by the end of the century, the convective environments are increasingly characterized by higher average CAPE ($\sim$ 400 Jkg^{-1}) and lower (more) average CIN ($\sim$ -80 Jkg^{-1}) supportive of more vigorous convection, but a stronger capping inversion.

Building on this, we have taken a similar approach using the CESM2-LE and found large agreements in our results for MAMJ CAPE versus CIN (Figure 3.7a). The advantage of this analysis is that it illustrates changes in both the forced and internal components of the convective indices as they evolve in time. The historical climatology (1971-2000 in blue) and future 30-year periods (2021-2050 in orange; and 2071-2100 in green) illustrate the general trend of the forced response through time and the implied changes in convective modes and their frequency. Individual, or marginal, distributions are displayed on the opposite axis for each index, helping to highlight the range due to internal variability, and how it changes through the century. While the shape of the distribution gives some insight into the range of internal variability, the shifts in the CAPE versus CIN pattern as a whole are due to the changes in the forced response as a function of time.

For the late 20^{th} century (blue), the distribution in Figure 3.7a has the highest density of ensemble members around CAPE values of 440 Jkg^{-1} and CIN values around -29 Jkg^{-1}. Over the next several decades (orange), the distribution exhibits an overall shift toward the bottom right with relatively higher CAPE (560 Jkg^{-1}) and relatively lower CIN (-36 Jkg^{-1}). By the end of the 21^{st} century (green), the CAPE versus CIN distribution has shifted to higher CAPE and lower CIN, with average magnitudes of $\sim$ 745 Jkg^{-1} and -40 Jkg^{-1}, respectively (Figure 3.7a). As mentioned, the shape of the epochs gives us insight into the range of outcomes associated with the internal climate variability. In Figure 3.7a, the shape of the end-of-century epoch (green) indicates that the future projections of CAPE could be anywhere from approximately 500 to 1050 Jkg^{-1} by the end of the century. Conversely, even with an ensemble mode of -40 Jkg^{-1}, the range of future projections for CIN due to the internal variability could fall anywhere between -26 and -70 Jkg^{-1} (Figure 3.7a). Thus, even though a wide range of plausible outcomes exist for both CAPE and CIN due to the role of internal variability, a majority of the ensembles suggest future environ-

ments over the southeastern CONUS composed of high CAPE and moderate CIN. These results further support the notion that strong, explosive convection is likely to increase in frequency, while weak-moderate convection is likely to be less supported (Diffenbaugh et al. 2013; Rasmussen et al. 2017; Lepore et al. 2021). The balance between these two thermodynamic indices is key to determining future convective modes and frequency (Rasmussen et al. 2017; Chen et al. 2020; Diffenbaugh et al. 2013; Lepore et al. 2021).

The same analysis can be completed to better understand changes in the CAPE and S06 phase space, which is critical for storm type and organization (Figure 3.7b). Overall, the distribution of these two indices shifts from relatively moderate CAPE and high S06 to higher CAPE and lower S06. The CAPE distributions are the same from Figure 3.7a, but the distribution in bulk wind shear follows a decreasing trend throughout the century, with an ensemble mode of approximately 14.5 ms^{-1} by 2100 (Figure 3.7b, green). Although, as with CAPE versus CIN, the role of internal variability is illustrated by the shape of each of these epochs. It is clear that from the historical climatology to the end of the century, the shape of the epochs evolves from long and narrow to a more circular shape. This indicates that future magnitudes of S06 are robust across all members and that while the internal variability plays a role in modulating the range of this decrease, the likelihood of environments being composed of decreasing wind shear is high. These results support previous findings of future environments abundant in energy for convection but with decreased wind shear (Trapp et al. 2007; Diffenbaugh et al. 2013; Hoogewind et al. 2017; Lepore et al. 2021).

Previously, Brooks et al. (2013) analyzed soundings produced by reanalysis data that were associated with severe thunderstorms in the U.S. from 1997-1999. These soundings were further classified as little severe, significant severe, and significant tornadoes. Their two-dimensional histogram of CAPE and S06 indicated the most severe storms were characterized by high CAPE and high wind shear (i.e., the top right of Figure 3.7b). Further, the storms that were classified as significant tornadoes had S06 greater than 10 ms^{-1}, and storms that were classified as significant severe exhibited S06 greater than 5 ms^{-1}. The distribution for significant severe storms existed over the high CAPE region (100-5,000 Jkg^{-1}), but significant tornadoes exhibited values across

the full range of CAPE distributions.

Comparing our results to the storm classifications in Brooks et al. (2003) and other studies (Rasmussen and Blanchard 1998; Brooks 2009), the projected increases in end-of-century CAPE will be more than sufficient to support significant severe storms and tornadoes. Further, while S06 is projected to decrease, even in the presence of internal variability, the absolute magnitudes of wind shear (Figure 3.7b) remain above the threshold to produce significant severe weather, but may not be as supportive of the most intense types of severe weather (i.e. tornadoes). The implication of higher CAPE and lower S06 is that when future storms do occur, there is a smaller chance that they will have the necessary dynamical support to produce the most intense severe weather, compared to the current climate, paralleling past research (Diffenbaugh et al. 2013; Lepore et al. 2021).

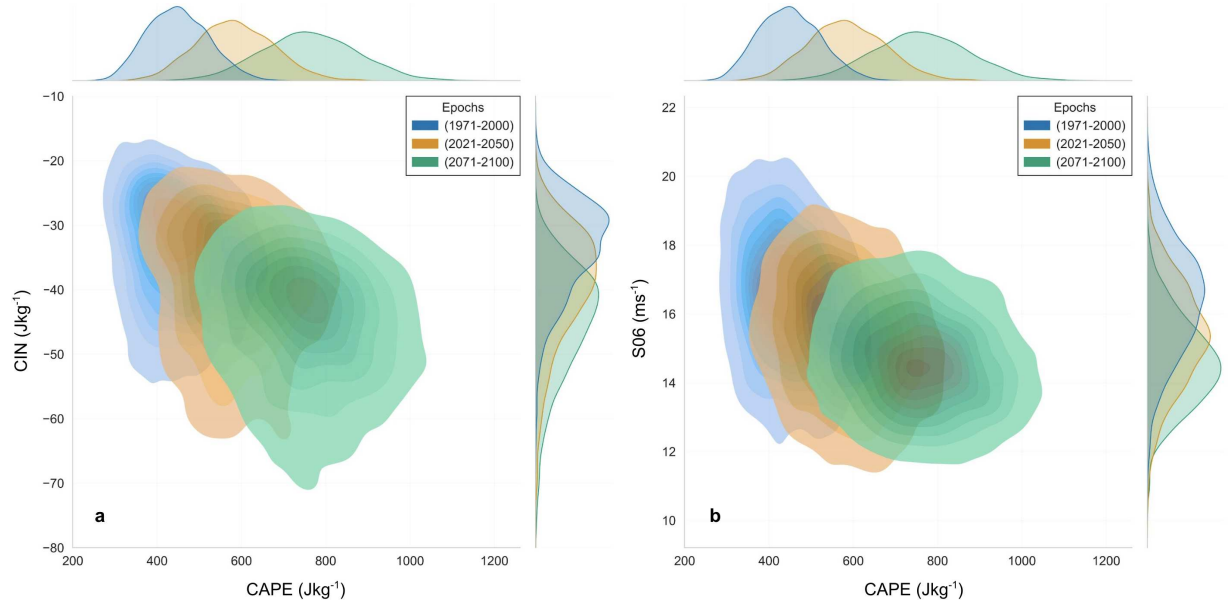

Figure 3.7: Bivariate distributions over eastern CONUS for MAMJ (A) CAPE (Jkg^{-1}) vs. CIN (Jkg^{-1}) and (B) CAPE (Jkg^{-1}) vs. S06 (ms^{-1}) for various epochs: 1971-2000 in blue, 2021-2050 in orange, and 2071-2100 in green. Marginal distributions for each index and period are shown on the opposite axis.

Chapter 4

Conclusion

4.1 Summary

An important goal of this study was to better understand how severe and hazardous weather is likely to change in a warmer climate. While the spatiotemporal scales on which severe storms form are smaller than can be explicitly resolved by relatively coarse resolution models such as the CESM2-LE, such models can be leveraged to instead examine the evolution of the large-scale convective environments in which the storms develop. Further, by using a large ensemble of climate model simulations as we have done with the CESM2-LE, it is possible to not only identify and examine robust, anthropogenically-forced changes in convective environments over time, but also examine how the forced changes are likely to be altered by internal climate variability, which to our knowledge, has yet to be explored. An increased understanding of the range of plausible, future convective environments and their corresponding uncertainties will enhance our capability to better project the nature of severe weather in the future, and perhaps increase resilience to these hazards.

Our study is novel in that we have examined the continuous-time evolution of various convective indices from 1870-2100 over the CONUS using a 50-member ensemble from a well-documented and understood Earth system model. Furthermore, by using a large-ensemble from a single model, we were able to help reduce future uncertainty in these environments and obtain a more robust estimate of the forced response than has previously been done before, as well as examine the plausible range of this response. Our results largely support the findings from previous studies that future convective environments over the eastern CONUS are likely to be characterized by less frequent, but more explosive and deep convection. However, there will be less kinematic support, which means less support for the organization of supercells capable of delivering the most extreme severe weather risks.

As discussed in the introduction, it is clear that severe weather hazards in the eastern U.S. have become a greater threat over the past few decades. Therefore, having the most complete knowledge of future changes in the these environments is paramount for things like climate adaptation policies and increasing overall future resilience to these hazards. Yet again, by taking advantage of a large-ensemble approach, we were able to investigate the effect of internal climate variability on large-scale convective environments, rather than just the forced response as most previous studies have done. This has helped to shed greater insight into the uncertainty in the range of future convective environments, which is yet another novelty of this work. While we have shown that the end-of-century changes in convective environments due to the forced response are spatially coherent and robust, we also exemplified how these changes can be modulated by the internal variability in such a way that acts to suppress and completely counteract the positive forced changes. We have also demonstrated that the opposite is also possible and that by 2050, the internal variability could enhance the forced changes of these proxies and yield convective environments more supportive of severe weather outbreaks. The key point is that the CESM2-LE has provided us the opportunity to examine a total of 50 different realizations of future large-scale convective environments over eastern CONUS, each of which is equally plausible.

Examining the convective proxies and the bivariate distributions of the selected indices, it is likely that future environments will be characterized by high CAPE, moderate-high CIN, and low S06. This type of environment is often conducive to less frequent but more intense convection and further, lacking the kinematic support needed for the most severe weather risks. Thus, our results suggest that there will be an increase in frequency in the less severe convective modes such as multicellular thunderstorms. The actual time evolution of these quantities will, of course, not only be influenced by forced climate change, but also by internal variations. While it is not possible to make a deterministic prediction of how actual convective environments over the CONUS will evolve throughout the rest of this century using this model, our study has helped to quantify the range of plausible scenarios, which are novel results.

Thus, the salient point is that throughout the century, changes in convective environments will likely manifest into an increase in the number of severe weather days during the MAMJ season over the eastern U.S.

This conclusion depends on the assumption that the CESM2-LE is capable of accurately simulating the future, even though it performs well in simulating past convective environments (e.g., Figure 2.2 and Figure 2.3). Our results are also dependent on the future forcing scenario (SSP3-7.0) used to produce the CESM2-LE which remains the chief source of uncertainty in future projections. Enhanced understanding of possible future changes in large-scale convective environments remains a key element for understanding future changes in the hazards associated with severe weather as well as how we choose to adapt to these hazards.

4.2 Future Work

Our study is the first to exploit the CESM2-LE to examine changes in convective parameters. Plans for future work include a more comprehensive regional analyses into sub domains within the eastern CONUS region (Figure 2.1), in order to obtain a more fine-scale representation of the internal variability, especially since some regions are less influenced by internal variability than others (Deser et al. 2012a). Also, given the pronounced role of internal variability over the southeastern U.S., further analysis is necessary to examine the large-scale circulation changes that drive internal variations in the convective indices, and if those circulation changes are connected to large-scale coupled modes of climate variability. If so, it will be important to determine the level of predictability associated with the internal variability. Finally, we are also conducting similar analyses for other seasons, as well as other regions of the world where convective activity is pronounced, such as over Argentina, on the lee-side of the Andes (e.g., Mulhalland et al. 2019; Nesbitt et al. 2021).

References

Allen, J. T., Tippett, M. K., & Sobel, A. H. (2015). Influence of the El Niño/Southern Oscillation on tornado and hail frequency in the United States. *Nature Geosci*, *8*(4), 278–283. doi: 10.1038/ngeo2385

Brooks, H. (2009). Proximity soundings for severe convection for Europe and the United States from reanalysis data. *Atmospheric Research - ATMOS RES*, *93*, 546–553. doi: 10.1016/j.atmosres.2008.10.005

Brooks, H. E., Lee, J. W., & Craven, J. P. (2003). The spatial distribution of severe thunderstorm and tornado environments from global reanalysis data. *Atmospheric Research*, *67-68*, 73–94. doi: 10.1016/S0169-8095(03)00045-0

Capotondi, A., Deser, C., Phillips, A. S., Okumura, Y., & Larson, S. M. (2020). ENSO and Pacific Decadal Variability in the Community Earth System Model Version 2. *Journal of Advances in Modeling Earth Systems*, *12*(12), e2019MS002022. doi: 10.1029/2019MS002022

Carlson, T. N., Benjamin, S. G., Forbes, G. S., & Li, Y.-F. (1983). Elevated Mixed Layers in the Regional Severe Storm Environment: Conceptual Model and Case Studies. *Monthly Weather Review*, *111*(7), 1453–1474. doi: 10.1175/1520-0493(1983)111<1453:EMLITR>2.0.CO;2

Chen, J., Dai, A., Zhang, Y., & Rasmussen, K. L. (2020). Changes in Convective Available Potential Energy and Convective Inhibition under Global Warming. *Journal of Climate*, *33*(6), 2025–2050. doi: 10.1175/JCLI-D-19-0461.1

Colby, F. P. (1984). Convective Inhibition as a Predictor of Convection during AVE-SESAME II. *Monthly Weather Review*, *112*(11), 2239–2252. doi: 10.1175/1520-0493(1984)112<2239:CIAAPO>2.0.CO;2

Craven, J. P., & Brooks, H. E. (2004). Baseline Climatology of Sounding Derived Parameters Associated With Deep Moist Convection. *National Weather Digest*, *28*, 12.

Craven, J. P., Jewell, R. E., & Brooks, H. E. (2002). Comparison between Observed Convective Cloud-Base Heights and Lifting Condensation Level for Two Different Lifted Parcels.

Weather and Forecasting, *17*(4), 885–890. doi: 10.1175/1520-0434(2002)017<0885:CBOCCB>2.0.CO;2

Dai, A., Fung, I. Y., & Genio, A. D. D. (1997). Surface Observed Global Land Precipitation Variations during 1900–88. *Journal of Climate*, *10*(11), 2943–2962. doi: 10.1175/1520-0442(1997)010<2943:SOGLPV>2.0.CO;2

Dai, A., & Wigley, T. M. L. (2000). Global patterns of ENSO-induced precipitation. *Geophysical Research Letters*, *27*(9), 1283–1286. doi: 10.1029/1999GL011140

Danabasoglu, G., Lamarque, J.-F., Bacmeister, J., Bailey, D. A., DuVivier, A. K., Edwards, J., ... Strand, W. G. (2020). The Community Earth System Model Version 2 (CESM2). *Journal of Advances in Modeling Earth Systems*, *12*(2), e2019MS001916. doi: 10.1029/2019MS001916

Deser, C. (2020). "Certain Uncertainty: The Role of Internal Climate Variability in Projections of Regional Climate Change and Risk Management". *Earth's Future*, *8*(12), e2020EF001854. doi: 10.1029/2020EF001854

Deser, C., Knutti, R., Solomon, S., & Phillips, A. S. (2012a). Communication of the role of natural variability in future North American climate. *Nature Clim Change*, *2*(11), 775–779. doi: 10.1038/nclimate1562

Deser, C., Phillips, A., Bourdette, V., & Teng, H. (2012b). Uncertainty in climate change projections: the role of internal variability. *Clim Dyn*, *38*(3), 527–546. doi: 10.1007/s00382-010-0977-x

Diffenbaugh, N. S., Scherer, M., & Trapp, R. J. (2013). Robust increases in severe thunderstorm environments in response to greenhouse forcing. *Proceedings of the National Academy of Sciences*, *110*(41), 16361–16366. doi: 10.1073/pnas.1307758110

Eyring, V., Bony, S., Meehl, G. A., Senior, C. A., Stevens, B., Stouffer, R. J., & Taylor, K. E. (2016). Overview of the Coupled Model Intercomparison Project Phase 6 (CMIP6) experimental design and organization. *Geoscientific Model Development*, *9*(5), 1937–1958. doi: 10.5194/gmd-9-1937-2016

Gensini, V. A., & Ashley, W. S. (2011). Climatology of Potentially Severe Convective Environments from the North American Regional Reanalysis. , 40.

Golaz, J.-C., Larson, V. E., & Cotton, W. R. (2002). A PDF-Based Model for Boundary Layer Clouds. Part I: Method and Model Description. *Journal of the Atmospheric Sciences*, *59*(24), 3540–3551. doi: 10.1175/1520-0469(2002)059<3540:APBMFB>2.0.CO;2

Hawkins, E., & Sutton, R. (2009). The Potential to Narrow Uncertainty in Regional Climate Predictions. *Bulletin of the American Meteorological Society*, *90*(8), 1095–1108. doi: 10.1175/2009BAMS2607.1

Hersbach, H., Bell, B., Berrisford, P., Hirahara, S., Horányi, A., Muñoz-Sabater, J., ... Thépaut, J.-N. (2020). The ERA5 global reanalysis. *Quarterly Journal of the Royal Meteorological Society*, *146*(730), 1999–2049. doi: 10.1002/qj.3803

Higgins, R. W., Yao, Y., Yarosh, E. S., Janowiak, J. E., & Mo, K. C. (1997). Influence of the Great Plains Low-Level Jet on Summertime Precipitation and Moisture Transport over the Central United States. *Journal of Climate*, *10*(3), 481–507. doi: 10.1175/1520-0442(1997)010<0481:IOTGPL>2.0.CO;2

Holton, J. R. (1972). *An introduction to dynamic meteorology* (No. 16). New York: Academic Press.

Hoogewind, K. A., Baldwin, M. E., & Trapp, R. J. (2017). The Impact of Climate Change on Hazardous Convective Weather in the United States: Insight from High-Resolution Dynamical Downscaling. *Journal of Climate*, *30*(24), 10081–10100. doi: 10.1175/JCLI-D-16-0885.1

Hurrell, J. W., Holland, M. M., Gent, P. R., Ghan, S., Kay, J. E., Kushner, P. J., ... Marshall, S. (2013). The Community Earth System Model: A Framework for Collaborative Research. *Bulletin of the American Meteorological Society*, *94*(9), 1339–1360. doi: 10.1175/BAMS-D-12-00121.1

Johns, R. H., & Doswell, C. A. (1992). Severe Local Storms Forecasting. *Weather and Forecasting*, *7*(4), 588–612. doi: 10.1175/1520-0434(1992)007<0588:SLSF>2.0.CO;2

Jorgensen, D. P., & Weckwerth, T. M. (2003). Forcing and Organization of Convective Systems.

In R. M. Wakimoto & R. Srivastava (Eds.), *Radar and Atmospheric Science: A Collection of Essays in Honor of David Atlas* (pp. 75–103). Boston, MA: American Meteorological Society.

Kelly, D. L., Schaefer, J. T., & Doswell, C. A. (1985). Climatology of Nontornadic Severe Thunderstorm Events in the United States. *Monthly Weather Review*, *113*(11), 1997–2014. doi: 10.1175/1520-0493(1985)113<1997:CONSTE>2.0.CO;2

Kirtman, B. P., Min, D., Infanti, J. M., Kinter, J. L., Paolino, D. A., Zhang, Q., ... Wood, E. F. (2014). The North American Multimodel Ensemble: Phase-1 Seasonal-to-Interannual Prediction; Phase-2 toward Developing Intraseasonal Prediction. *Bulletin of the American Meteorological Society*, *95*(4), 585–601. doi: 10.1175/BAMS-D-12-00050.1

Klemp, J. (2003). Dynamics Of Tornadic Thunderstorms. *Annual Review of Fluid Mechanics*, *19*, 369–402. doi: 10.1146/annurev.fl.19.010187.002101

Lee, S.-K., Atlas, R., Enfield, D., Wang, C., & Liu, H. (2013). Is There an Optimal ENSO Pattern That Enhances Large-Scale Atmospheric Processes Conducive to Tornado Outbreaks in the United States? *Journal of Climate*, *26*(5), 1626–1642. doi: 10.1175/JCLI-D-12-00128.1

Lepore, C., Abernathey, R., Henderson, N., Allen, J. T., & Tippett, M. K. (2021). Future Global Convective Environments in CMIP6 Models. *Earth's Future*, *9*(12), e2021EF002277. doi: 10.1029/2021EF002277

Li, F., Chavas, D. R., Reed, K. A., & Ii, D. T. D. (2020). Climatology of Severe Local Storm Environments and Synoptic-Scale Features over North America in ERA5 Reanalysis and CAM6 Simulation. *Journal of Climate*, *33*(19), 8339–8365. doi: 10.1175/JCLI-D-19-0986.1

Li, W., Li, L., Fu, R., Deng, Y., & Wang, H. (2011). Changes to the North Atlantic Subtropical High and Its Role in the Intensification of Summer Rainfall Variability in the Southeastern United States. *Journal of Climate*, *24*(5), 1499–1506. doi: 10.1175/2010JCLI3829.1

Lilly, D. K. (1979). The Dynamical Structure and Evolution of Thunderstorms and Squall Lines. *Annual Review of Earth and Planetary Sciences*, *7*, 117. doi: 10.1146/annurev.ea.07.050179

.001001

Ludlam, F. H. (1963). Severe Local Storms: A Review. In D. Atlas et al. (Eds.), *Severe Local Storms* (pp. 1–32). Boston, MA: American Meteorological Society.

Mankin, J. S., Lehner, F., Coats, S., & McKinnon, K. A. (2020). The Value of Initial Condition Large Ensembles to Robust Adaptation Decision-Making. *Earth's Future*, *8*(10), e2012EF001610. doi: 10.1029/2020EF001610

Milinski, S., Maher, N., & Olonscheck, D. (2020). How large does a large ensemble need to be? *Earth System Dynamics*, *11*(4), 885–901. doi: 10.5194/esd-11-885-2020

Mulholland, J. P., Nesbitt, S. W., Trapp, R. J., Rasmussen, K. L., & Salio, P. V. (2018). Convective Storm Life Cycle and Environments near the Sierras de Córdoba, Argentina. *Monthly Weather Review*, *146*(8), 2541–2557. doi: 10.1175/MWR-D-18-0081.1

NCEI. (2021). *U.S. Billion-dollar Weather and Climate Disasters, 1980 - present (NCEI Accession 0209268).*

Neale, R. B., & Gettelman, A. (2012). *Description of the NCAR Community Atmosphere Model (CAM 5.0)* (Tech. Rep.). NCAR/UCAR.

Nesbitt, S. W., Salio, P. V., Ávila, E., Bitzer, P., Carey, L., Chandrasekar, V., ... Grover, M. A. (2021). A Storm Safari in Subtropical South America: Proyecto RELAMPAGO. *Bulletin of the American Meteorological Society*, *102*(8), E1621–E1644. doi: 10.1175/BAMS-D-20-0029.1

O'Neill, B. C., Tebaldi, C., van Vuuren, D. P., Eyring, V., Friedlingstein, P., Hurtt, G., ... Sanderson, B. M. (2016). The Scenario Model Intercomparison Project (ScenarioMIP) for CMIP6. *Geoscientific Model Development*, *9*(9), 3461–3482. doi: 10.5194/gmd-9-3461-2016

Otto-Bliesner, B. L., Brady, E. C., Fasullo, J., Jahn, A., Landrum, L., Stevenson, S., ... Strand, G. (2016). Climate Variability and Change since 850 CE: An Ensemble Approach with the Community Earth System Model. *Bulletin of the American Meteorological Society*, *97*(5), 735–754. doi: 10.1175/BAMS-D-14-00233.1

Pitchford, K. L., & London, J. (1962). The Low-Level Jet as Related to Nocturnal Thunderstorms

over Midwest United States. *Journal of Applied Meteorology and Climatology*, *1*(1), 43–47. doi: 10.1175/1520-0450(1962)001<0043:TLLJAR>2.0.CO;2

Powers, J. G., Klemp, J. B., Skamarock, W. C., Davis, C. A., Dudhia, J., Gill, D. O., ... Duda, M. G. (2017). The Weather Research and Forecasting Model: Overview, System Efforts, and Future Directions. *Bulletin of the American Meteorological Society*, *98*(8), 1717–1737. doi: 10.1175/BAMS-D-15-00308.1

Rasmussen, E. N., & Blanchard, D. O. (1998). A Baseline Climatology of Sounding-Derived Supercell and Tornado Forecast Parameters. *Weather and Forecasting*, *13*(4), 1148–1164. doi: 10.1175/1520-0434(1998)013<1148:ABCOSD>2.0.CO;2

Rasmussen, K. L., Prein, A. F., Rasmussen, R. M., Ikeda, K., & Liu, C. (2017). Changes in the convective population and thermodynamic environments in convection-permitting regional climate simulations over the United States. *Clim Dyn*, *55*(1), 383–408. doi: 10.1007/s00382-017-4000-7

Riemann-Campe, K., Fraedrich, K., & Lunkeit, F. (2009). Global climatology of Convective Available Potential Energy (CAPE) and Convective Inhibition (CIN) in ERA-40 reanalysis. *Atmospheric Research*, *93*(1), 534–545. doi: 10.1016/j.atmosres.2008.09.037

Rochette, S. M., Moore, J. T., & Market, P. S. (1999). The importance of parcel choice in elevated CAPE computations. *Natl. Wea. Dig*, *23*(4), 20–32.

Rodgers, K. B., Lee, S.-S., Rosenbloom, N., Timmermann, A., Danabasoglu, G., Deser, C., ... Yeager, S. G. (2021). Ubiquity of human-induced changes in climate variability. *Earth System Dynamics*, *12*(4), 1393–1411. doi: 10.5194/esd-12-1393-2021

Ropelewski, C. F., & Halpert, M. S. (1986). North American Precipitation and Temperature Patterns Associated with the El Niño/Southern Oscillation (ENSO). *Monthly Weather Review*, *114*(12), 2352–2362. doi: 10.1175/1520-0493(1986)114<2352:NAPATP>2.0.CO;2

Rotunno, R. (1981). On the Evolution of Thunderstorm Rotation. *Monthly Weather Review*, *109*(3), 577–586. doi: 10.1175/1520-0493(1981)109<0577:OTEOTR>2.0.CO;2

Seeley, J. T., & Romps, D. M. (2015). The Effect of Global Warming on Severe Thunderstorms in

the United States. *Journal of Climate*, *28*(6), 2443–2458. doi: 10.1175/JCLI-D-14-00382.1

Taszarek, M., Allen, J. T., Marchio, M., & Brooks, H. E. (2021). Global climatology and trends in convective environments from ERA5 and rawinsonde data. *npj Clim Atmos Sci*, *4*(1), 1–11. doi: 10.1038/s41612-021-00190-x

Taylor, K. E., Stouffer, R. J., & Meehl, G. A. (2012). An Overview of CMIP5 and the Experiment Design. *Bulletin of the American Meteorological Society*, *93*(4), 485–498. doi: 10.1175/BAMS-D-11-00094.1

Thompson, D. B., & Roundy, P. E. (2013). The Relationship between the Madden–Julian Oscillation and U.S. Violent Tornado Outbreaks in the Spring. *Monthly Weather Review*, *141*(6), 2087–2095. doi: 10.1175/MWR-D-12-00173.1

Ting, M., Kossin, J. P., Camargo, S. J., & Li, C. (2019). Past and Future Hurricane Intensity Change along the U.S. East Coast. *Sci Rep*, *9*(1), 7795. doi: 10.1038/s41598-019-44252-w

Trapp, R. J., Diffenbaugh, N. S., Brooks, H. E., Baldwin, M. E., Robinson, E. D., & Pal, J. S. (2007). Changes in severe thunderstorm environment frequency during the 21st century caused by anthropogenically enhanced global radiative forcing. *Proceedings of the National Academy of Sciences*, *104*(50), 19719–19723. doi: 10.1073/pnas.0705494104

Trapp, R. J., Diffenbaugh, N. S., & Gluhovsky, A. (2009). Transient response of severe thunderstorm forcing to elevated greenhouse gas concentrations. *Geophysical Research Letters*, *36*(1). doi: 10.1029/2008GL036203

Weisman, M. L., & Rotunno, R. (2000). The Use of Vertical Wind Shear versus Helicity in Interpreting Supercell Dynamics. *Journal of the Atmospheric Sciences*, *57*(9), 1452–1472. doi: 10.1175/1520-0469(2000)057<1452:TUOVWS>2.0.CO;2

Zhang, G., & McFarlane, N. A. (1995). Sensitivity of climate simulations to the parameterization of cumulus convection in the Canadian climate centre general circulation model. *Atmosphere-Ocean*, *33*(3), 407–446. doi: 10.1080/07055900.1995.9649539

Appendix A

Supplemental Material

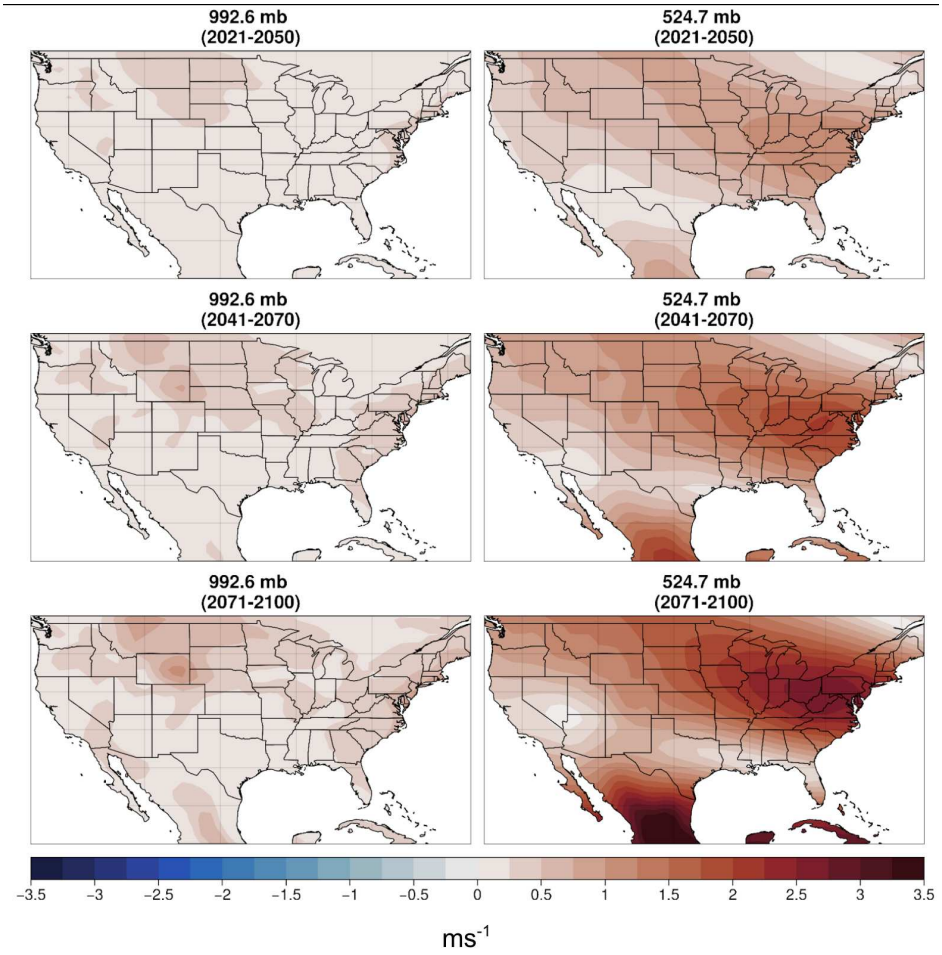

Figure A.1: Full wind anomalies (ms^{-1}) from the 1971-2000 climatology. 10-meter surface winds ($\sim$ 993-mb) on the left and 6-km upper-level winds ($\sim$ 525-mb) on the right.

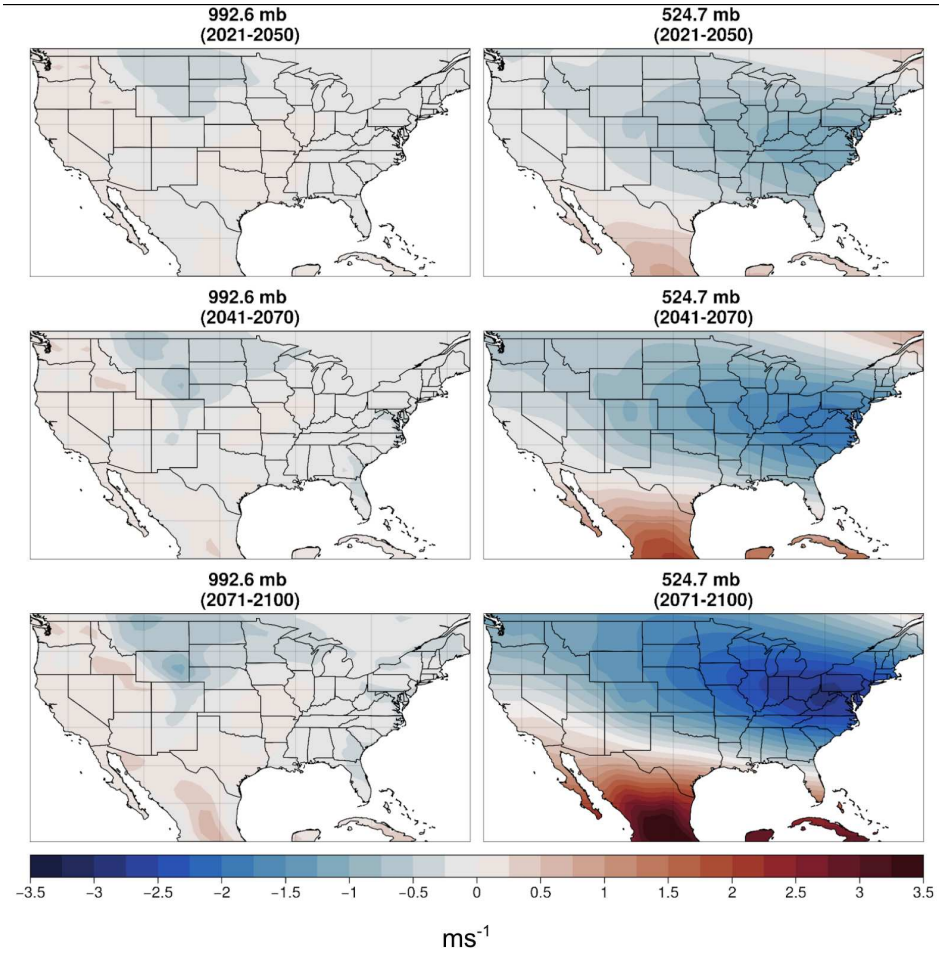

Figure A.2: Zonal wind anomalies (ms^{-1}) from the 1971-2000 climatology. 10-meter surface winds ($\sim$ 993-mb) on the left and 6-km upper-level winds ($\sim$ 525-mb) on the right.

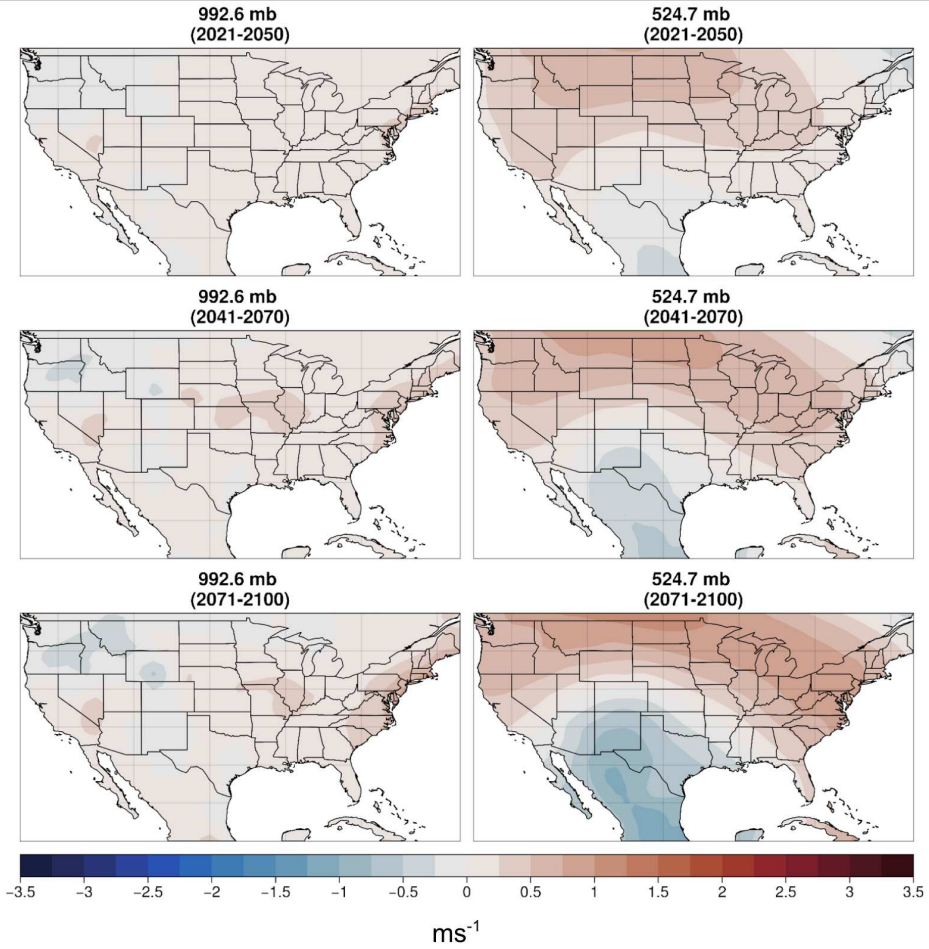

Figure A.3: Meridional wind anomalies (ms^{-1}) from the 1971-2000 climatology. 10-meter surface winds ($\sim$ 993-mb) on the left and 6-km upper-level winds ($\sim$ 525-mb) on the right.